

Smooth Conformal Surface for Genus-0 manifold

Cheng-Yuan Liou, Yen-Ting Kuo, and Jau-Chi Huang

Department of Computer Science and

Information Engineering

National Taiwan University

Taipei, Taiwan

Email: cylie@csie.ntu.edu.tw

Supported by NSC 93-2213-E-002-008

September 30, 2005

Abstract. This paper presents a method to construct a smooth seamless conformal surface for the genus-0 manifold. The constructed surface is both smooth and continuous. This method is developed from the conformal self-organizing map [14]. The mapping between the model surface and the sphere surface is one-to-one and onto. We show experiments in texture mapping and compare it with other methods.

Keywords: surface construction, smooth seamless surface, conformal mapping, self-organizing map

1. Introduction

The goal of surface reconstruction is to obtain a continuous surface that can represent a cloud of pattern points [3]. These cloud patterns are

© 2005 Kluwer Academic Publishers. Printed in the Netherlands.

usually obtained from 3D laser scanners and medical scanners. These patterns may also be collected by various vision techniques, such as correlated viewpoints, voxel carving, stereo range images. Let X denote the set that contains all point patterns, $X = \{(x_l, y_l, z_l)^T, l = 1, \dots, P\}$. The conformal self-organizing map (CSM) [14][13] derives a continuous surface for the cloud patterns using a collection of connected simplices including points, edges, and triangles. It is a kind of self-organizing map [11] with conformal contents [12]. Since these triangles are flat, the surface constructed by these flat triangles will give a continuous surface but not give a curved smooth surface. In this paper we show how to construct a curved smooth seamless surface based on the derived surface by the CSM. We will also discuss the global conformal surface given in [6][5].

Let the surface of a collection of all triangles inside a unit sphere be S^Δ , $S^\Delta = \{\Delta_n^r, r = 1, \dots, R\}$, see Fig. 1(b). Let the collection of all vertices (nodes) be $\mathbb{N} = \{n_i, i = 1, \dots, N\}$, where n_i is a 3D column vector in the network space and contains the position of the i^{th} mesh vertex on the unit sphere surface. Each triangle is a mesh hole that can be represented by its three vertices, that is, $\Delta_n^r \equiv [n_i^r, n_j^r, n_k^r]$. An icosahedron dome is used to represent this sphere surface [10]. Each Δ_n^r is a face of the icosahedron and an equilateral triangle. The basic type of an icosahedron has 12 vertices, 30 edges, and 20 equivalent equilateral

triangular faces. It is varied by combining more icosahedrons into a single body. We use the term f (frequency) to denote its multiplicity.

The formula of the icosahedron is

$$\begin{aligned} R &= \text{the number of faces} = 20f^2, \\ N &= \text{the number of vertices} = \frac{R}{2} + 2. \end{aligned} \quad (1)$$

Review the CSM

In the CSM, the sampled 3D patterns are the training patterns and the mesh is configured by neurons. These neurons are the vertices of the mesh. Each neuron has two vectors, one is the weight vector, w_i , in the pattern space and the other is the position vector, n_i , in the network space. The weight vectors contain the locations of the mesh vertices in the pattern space. The position vectors contain the locations of the neurons on the sphere surface. Figure 1 shows the relationship of these two vectors. In the CSM, w_i is evolved to match its corresponding pattern and n_i is fixed to preserve the sphere topology.

The CSM constructs a mapping from S^Δ to M^Δ [14], where M^Δ is the manifold of the cloud patterns. M^Δ is the constructed model surface or the manifold surface to represent the cloud X . M^Δ is the surface formed by a collection of the flat triangles, $M^\Delta = \{\Delta_w^r, r =$

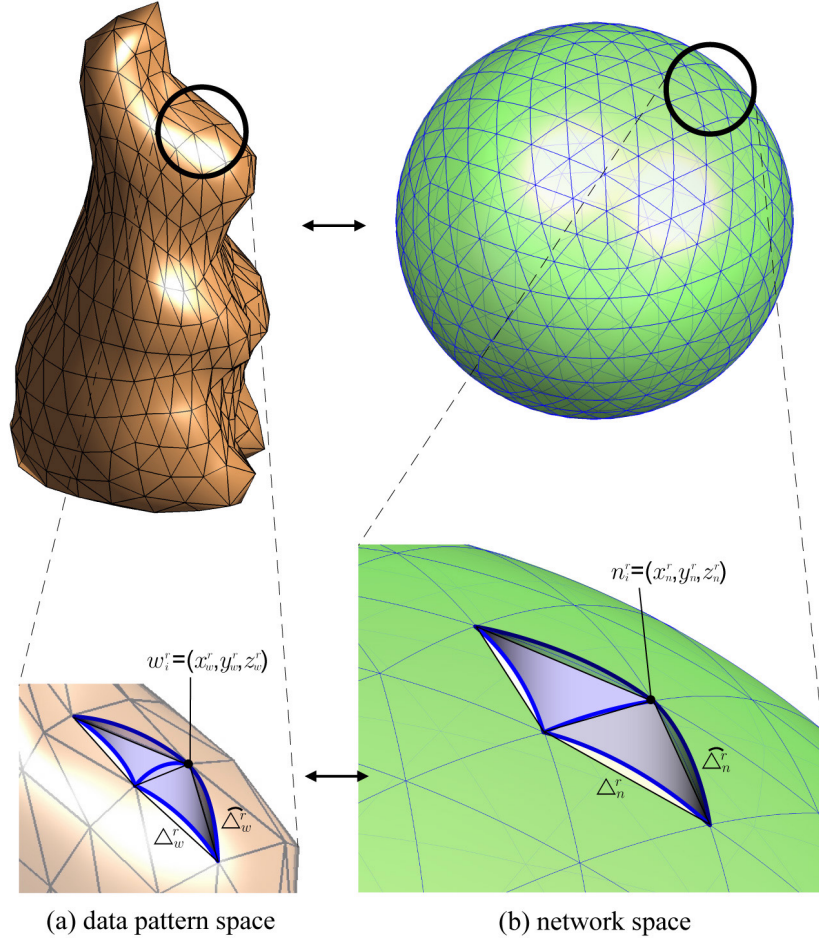


Illustration of the pattern space X and the network space in the CSM. (a) The patterns and the model surface are in the same space. (b) The position vectors are fixed as the vertices (or neurons) and arranged uniformly on the unit sphere surface. The weight vector and the position vector of the i^{th} neuron are marked with black dots in both space. w_i^r and n_i^r are these two vectors. Each flat triangle Δ_w^r on the model surface can be mapped to its corresponding triangle Δ_n^r on the sphere surface. The triangular domes $\widehat{\Delta}_n^r$ and $\widehat{\Delta}_w^r$ of these two flat triangles are marked with thick blue arcs.

Figure 1.

$1, \dots, R\}$. By using the CSM, each equilateral triangle Δ_n^r is mapped to its corresponding triangle Δ_w^r . Δ_w^r is an irregular triangle and a mesh hole that can be represented by its three vertices, that is, $\Delta_w^r = [w_i^r, w_j^r, w_k^r]$, where w_i^r is a 3D column weight vector in the pattern space and contains the position of the i^{th} mesh vertex in M^Δ , see Fig. 1(a). The vertex w_i^r is mapped to the vertex n_i^r . Both Δ_w^r and Δ_n^r are flat triangles. In the CSM, the parameterization domain is the surface S^Δ which is suitable for the genus zero manifold. The set \mathbb{N} contains all joint points between S^Δ and the unit sphere surface, S .

There are ways to construct a smooth dome over the Δ_w^r , such as fitting a triangular surface spline. Since the sphere surface is both continuous and smooth, these beautiful properties are useful in building other surface. We show how to map (borrow) the sphere surface, S , to its corresponding model surface based on the derived M^Δ . The detailed method is in the next section. Experiments and discussions will be given in the Section 3.

2. Smooth conformal surface parameterization

By using the CSM [14], we can derive the M^Δ and obtain the mapping between each triangle Δ_n^r and its corresponding triangle Δ_w^r . Let the

portion of the sphere surface right above the flat triangle, Δ_n^r , be $\widehat{\Delta}_n^r$, see Fig. 1(b). The triangular dome $\widehat{\Delta}_n^r$ can be obtained by cutting the three arc curves, $\{\widehat{n}_i^r n_j^r, \widehat{n}_j^r n_k^r, \widehat{n}_i^r n_k^r\}$, on the sphere surface right above the three edges, $\{\overline{n_i^r n_j^r}, \overline{n_j^r n_k^r}, \overline{n_i^r n_k^r}\}$, of the triangle Δ_n^r . Each arc point is the intersection of the sphere surface and the line that passes through the sphere center, $c = (0, 0, 0)^T$, and an edge point. The arc $\widehat{n}_i^r n_j^r$, edge $\overline{n_i^r n_j^r}$, and center c are in the same plane. $\widehat{\Delta}_n^r$ is the geodesic dome of Δ_n^r and has a triangular tent shape. The sphere surface, S , is the collection of every $\widehat{\Delta}_n^r$, $S = \{\widehat{\Delta}_n^r, r = 1, \dots, R\}$. Since the dome $\widehat{\Delta}_n^r$ is beautiful that is both smooth and continuous, we want to borrow and fit (deform) the dome to construct a smooth model surface for the cloud X . In the following algorithm, we show how to map each $\widehat{\Delta}_n^r$ to its corresponding dome, $\widehat{\Delta}_w^r$, to obtain a smooth model surface, M , where $M = \{\widehat{\Delta}_w^r, r = 1, \dots, R\}$.

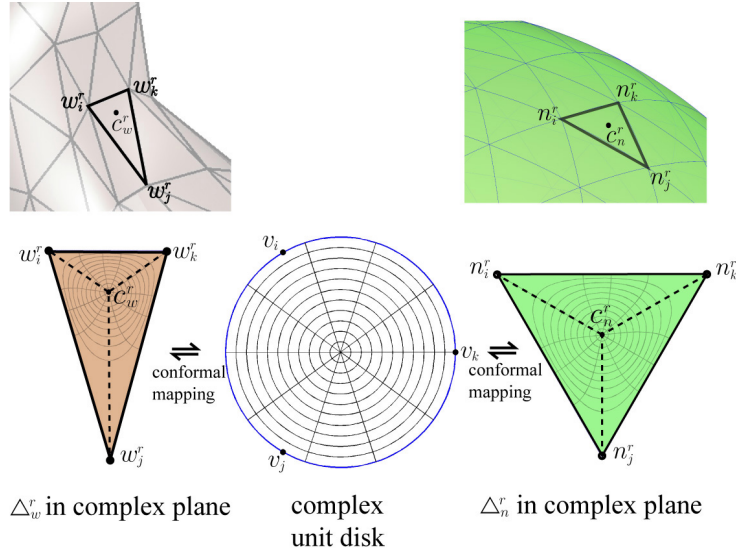
The algorithm to accomplish the $\widehat{\Delta}_w^r$ is in below.

Smooth Algorithm

Input: new dense mesh \mathbb{N}^{new} , sphere mesh S^Δ , model mesh M^Δ .

Output: smooth surface M .

1. For each triangle Δ_n^r , $\Delta_n^r \in S^\Delta$, find the center c_n^r of the triangle Δ_n^r and its conformal mapping point, c_w^r , in Δ_w^r , see Fig. 2.



Conformal mapping between the two triangles Δ_n^r and Δ_w^r . Each triangle in 3D is translated to the complex plane. Then their conformal mappings to a unit disk can be computed by the Schwarz–Christoffel method [15] to build the point correspondence.

Figure 2.

2. Separate $\Delta_w^r, \Delta_n^r \in M^\Delta$, into three subtriangles, $\{[c_w^r, w_i^r, w_j^r], [c_w^r, w_j^r, w_k^r], [c_w^r, w_i^r, w_k^r]\}$, by using the three line sections, $\{c_w^r w_i^r, \overline{c_w^r w_j^r}, \overline{c_w^r w_k^r}\}$, and the three edges, $\{\overline{w_i^r w_j^r}, \overline{w_j^r w_k^r}, \overline{w_i^r w_k^r}\}$.

3. Calculate the unit normal vector of the triangle plane Δ_w^r :

$$\hat{n}_w^r = \frac{(w_j^r - w_i^r) \times (w_k^r - w_i^r)}{|(w_j^r - w_i^r) \times (w_k^r - w_i^r)|}. \quad (2)$$

4. Let the triangle next to Δ_w^r in M^Δ that shares the edge $\overline{w_i^r w_j^r}$ is Δ_w^{r1} , that shares the edge $\overline{w_j^r w_k^r}$ is Δ_w^{r2} , that shares the edge $\overline{w_i^r w_k^r}$

is $\Delta_w^{r^3}$. Calculate the unit normal vectors of the three neighborhood triangles, $\Delta_w^{r^1}$, $\Delta_w^{r^2}$, $\Delta_w^{r^3}$, by using the same equation in the above step. Let the obtained normal vectors be $\hat{n}_w^{r^1}$, $\hat{n}_w^{r^2}$, and $\hat{n}_w^{r^3}$ respectively.

5. Calculate the unit normal vectors of the edges, $\overline{w_i^r w_j^r}$, $\overline{w_j^r w_k^r}$, and $\overline{w_i^r w_k^r}$:

$$\tilde{e}_w^{r^1} = \frac{\hat{n}_w^r + \hat{n}_w^{r^1}}{|\hat{n}_w^r + \hat{n}_w^{r^1}|}, \tilde{e}_w^{r^2} = \frac{\hat{n}_w^r + \hat{n}_w^{r^2}}{|\hat{n}_w^r + \hat{n}_w^{r^2}|}, \text{ and } \tilde{e}_w^{r^3} = \frac{\hat{n}_w^r + \hat{n}_w^{r^3}}{|\hat{n}_w^r + \hat{n}_w^{r^3}|}. \quad (3)$$

Note that $\tilde{e}_w^{r^1} \perp \overline{w_i^r w_j^r}$, $\tilde{e}_w^{r^2} \perp \overline{w_j^r w_k^r}$, and $\tilde{e}_w^{r^3} \perp \overline{w_i^r w_k^r}$.

6. Select a point p on $\widehat{\Delta}_n^r$, $p \in \mathbb{N}^{new}$. Find its projection, p' , on the flat triangle Δ_n^r :

$$p' \equiv \overline{pc} \cap \Delta_n^r. \quad (4)$$

Here $c = (0, 0, 0)^T$ is the center of the unit sphere and p' is the

intersection point of the line \overline{pc} and Δ_n^r , see Fig. 3(a).

7. For the point p' , calculate its conformal mapping point q' in Δ_w^r .

$$q' = \mathcal{M}_{\Delta_n^r}^{\Delta_w^r}(p') \quad (5)$$

$\mathcal{M}_{\Delta_n^r}^{\Delta_w^r}$ is the conformal mapping [14] from the flat triangle Δ_n^r to the flat triangle Δ_w^r , see Fig. 3(b). q' may fall in any one of the three subtriangles. Suppose q' is in the subtriangle $[c_w^r, w_i^r, w_j^r]$.

8. Calculate the projection point $b_{q'}$ of q' on the line section $\overline{w_i^r w_j^r}$. This means that $\overline{w_i^r w_j^r} \perp \overline{b_{q'} q'}$. Calculate the intersection point $a_{q'}$ of the line $\overline{b_{q'} q'}$ and one of the other two edges of the subtriangle $[c_w^r, w_i^r, w_j^r]$. The locations of $a_{q'}$ and $b_{q'}$ are shown in Fig. 4.

9. Calculate the unit direction $\widehat{n}_{q'}$ at the point q' :

$$\begin{aligned}\widehat{n}_{q'} &= \frac{\vec{n}_{q'}}{|\vec{n}_{q'}|}, \\ \vec{n}_{q'} &= \frac{|q' - a_{q'}|}{|b_{q'} - a_{q'}|} (\widehat{e}_w^{r1} - \widehat{n}_w^r) + \widehat{n}_w^r.\end{aligned}\quad (6)$$

Note that q' , $a_{q'}$, $b_{q'}$, and $\widehat{n}_{q'}$ are in the same plane. The two vectors \widehat{e}_w^{r1} and \widehat{n}_w^r in Fig. 4 which pass the points $b_{q'}$ and $a_{q'}$ separately are also in this plane.

10. In this step we plan to determine a point q , $q \in M$, for the dome $\widehat{\Delta}_w^r$ that is correspond to p . q is obtained from the dome height $|p - p'|$ and the unit direction $\widehat{n}_{q'}$. q can be obtained by

$$q = q' + |p - p'| \widehat{n}_{q'}.$$

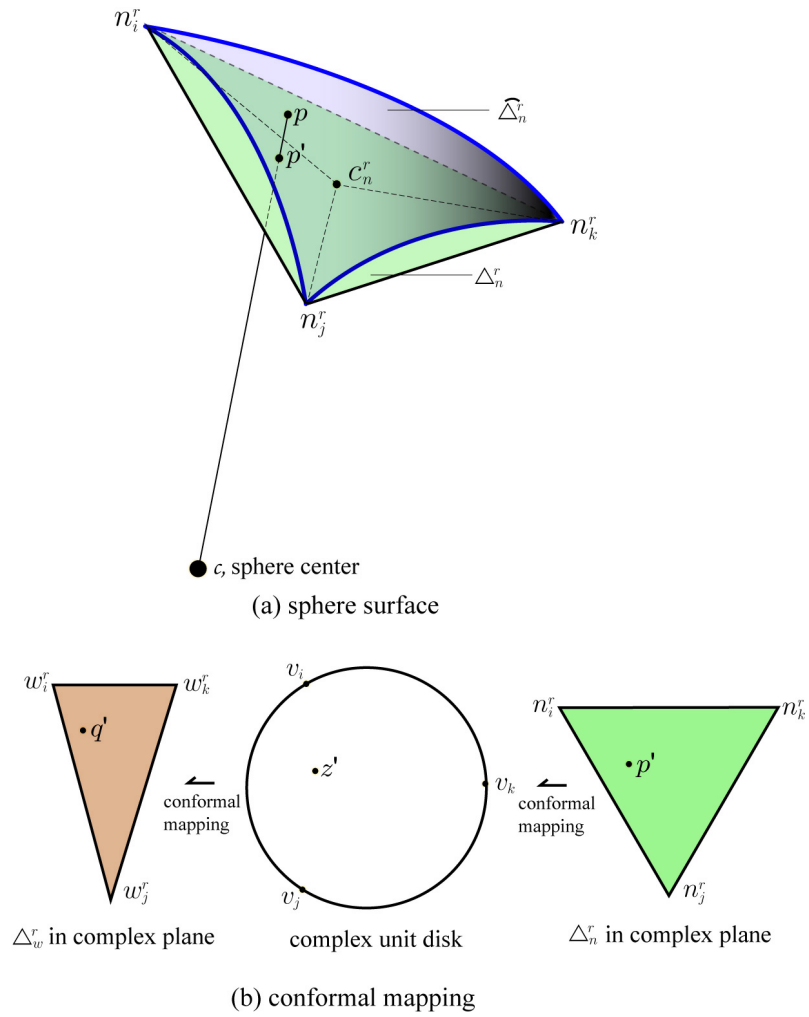
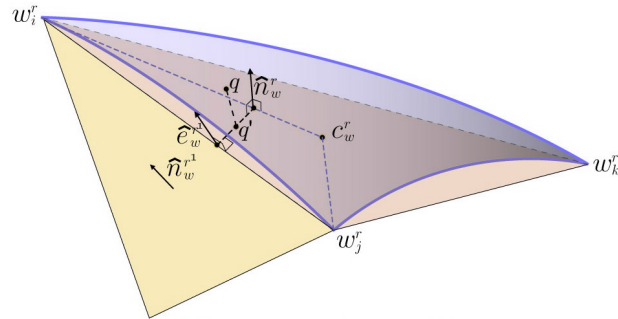


Illustration of the relations among the points p , p' , q' and c . (a) The intersection point p' on Δ_n^r is the joint point between the line \overline{pc} and Δ_n^r . (b) The point p' is then mapped to the point q' in Δ_w^r .

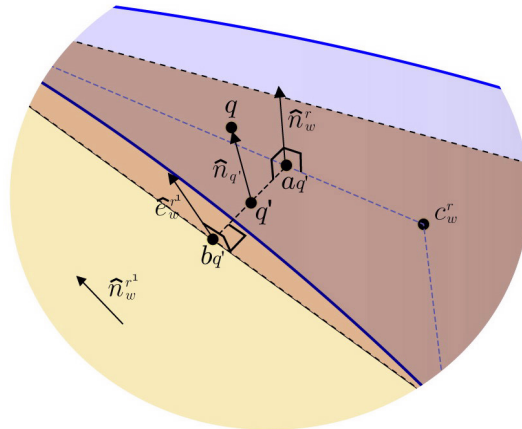
Figure 3.

The whole construction is shown in Figs. 3 and 4.

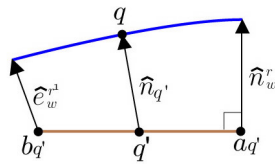
11. Go to step 6 and select another point, $p \in \mathbb{N}^{new}$, iteratively.



(a) mapped point q on $\widehat{\Delta}_w^r$



(b) magnified plot



(c) profile

Illustration of the relations between the points p and q . The direction of $\vec{n}_{q'}$ is a linear combination of \widehat{e}_w^{r1} and \widehat{n}_w^r . The height of the section $\overline{q'q}$ is the same as the height of $\overline{p'p}$.

Figure 4.

We operate this algorithm triangle after triangle for all R triangles. We may map any number of surface points for each triangle dome. This mapping is bijection which maps between the triangular sphere surface, $\widehat{\Delta}_n^r$, to the triangular geodesic model surface, $\widehat{\Delta}_w^r$. A point on the three boundary arc curves of $\widehat{\Delta}_w^r$ is continuous but may not be smooth. In all experiments, the surface point p on $\widehat{\Delta}_n^r$ is a vertice of a new denser mesh \mathbb{N}^{new} , where $N^{new} > N$. \mathbb{N}^{new} may be an icosahedron with more vertices. \mathbb{N}^{new} may have dense vertices in an area with fine texture.

3. Experiments

There are two models used in experiments including the Stanford bunny [20] and the Igea head [19]. Each one of them is used as the raw pattern cloud X_{raw} . The whole operation is in below.

1. Prepare pattern cloud of a model in $\{(x_l, y_l, z_l)_{raw}^T \in X_{raw}\}$ and prepare $S^\Delta = \{\Delta_n^r, r = 1, \dots, R\}$. Normalize this cloud in a unit cube by the formula

$$(x_l, y_l, z_l)^T = \frac{(x_l, y_l, z_l)_{raw}^T}{X_{raw}^{\max}},$$

where $X_{raw}^{\max} = \max\{x_l, y_l, z_l, l = 1, \dots, P\}$.

2. Operate the CSM and obtain the model surface with flat triangles

$$M^\Delta = \{\Delta_w^r, r = 1, \dots, R\}.$$

3. Construct a smooth model surface. Prepare a dense mesh \mathbb{N}^{new} on the sphere surface and apply the smooth algorithm to map its vertices on the model surface.

In certain case, such as the bunny data has long extrude parts, the ears, it is difficult for the CSM to learn those concave ear shapes. An edge swap with multi-resolution learning [18] and a growing neural mesh [8] may be used to overcome this difficulty. Since they change the regular mesh connection, we will not use them in the CSM. We solve this difficult learning by giving the priority to those extrude parts during the CSM learning. This priority can resolve those parts and keep the regular connection.

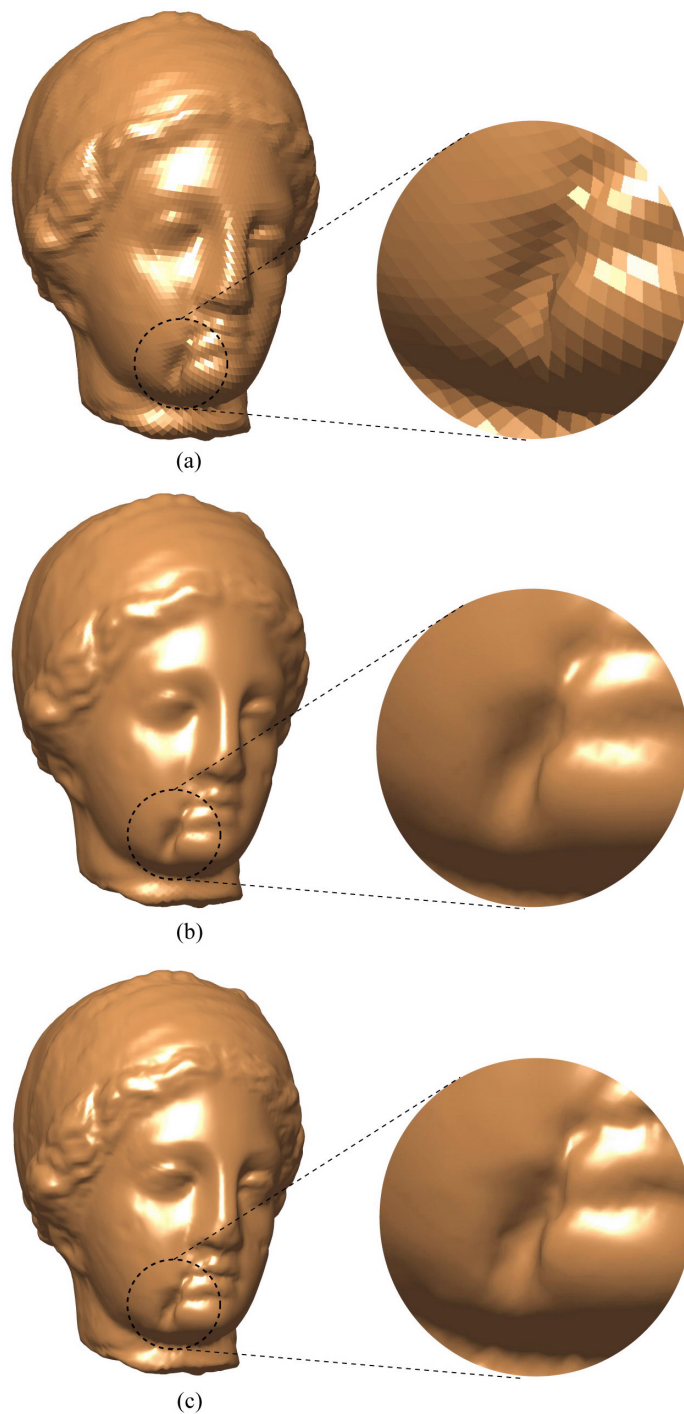
Smooth model surface

Figure 5 shows the constructed surface using the Igea head data. The total number of patterns is $P = 134345$. The mesh parameters in Figs. 5(a,b) are $R = 25920$, $f = 36$, and $N = 12962$. The model surface M^Δ obtained by the CSM is plotted in 5(a). In the CSM, we set the number of training epoch be $epoch = 80$. In each epoch, 8000 random sample patterns are used in the learning. The parameters for the neighborhood variance are set as $\sigma_0 = 0.4$ and $\tau_1 = 20$. The

parameters for the learning rate are set as $\alpha_0 \leftarrow 0.01$ and $\tau_2 \leftarrow 60$. The training parameters $epoch$, σ_0 , τ_1 , α_0 , and τ_2 are defined in [14]. We apply the shading method in [16] to the the mesh in Fig. 5(a) and obtain the image in Fig. 5(b). Figure 5(c) is the surface, M , constructed by using the proposed smooth algorithm. In Fig. 5(c) we map the vertices of a new mesh \mathbb{N}^{new} with parameters $R = 128000$, $f = 80$, and $N^{new} = 64002$. All 64002 vertices are mapped to the model surface by using the smooth algorithm.

Texture mapping

Part of the reason for building the smooth surface is to facilitate the texture mapping. One can trace the texture details equally on the smooth surface without any ambiguous correspondence. Figure 6(a) shows the smooth surface, M , using the Stanford bunny data. In this figure, the total number of patterns is $P = 35947$. We use the same training parameters and mesh parameters as those used in Fig. 5 to obtain the surface in Fig. 6(a). In Fig. 6(b), the checkerboard texture is mapped on the surface. This checkerboard, which is in a 2D plane, is first projected to the unit sphere surface, S , by using the stereographic projection [2]. Then, its sphere projection is mapped to the smooth model surface. The stereographic projection will generate serious distortion near the center of the projection. We use this projection is



(a) The Igea model surface M^Δ obtained by the CSM using $R = 25920$ faces. (b) The shading method in [16] is applied to M^Δ . (c) The smooth algorithm is applied to M^Δ with a denser mesh $N^{new} = 64002$ nodes.

Figure 5.

because it is a conformal mapping and is very regular near the point of tangency. A facial makeup of Chinese operas in Fig. 6(c) are mapped to the smooth surface by the same projection, see Fig. 6(d).

Figure 7 shows two texture mapping cases. Figures 7(a,b) show the checkerboard texture on the smooth Igea surface in Fig. 5(c). A facial makeup in Chinese opera in Fig. 7(c) is mapped on the smooth Igea surface, see Fig. 7(d).

Comparison with the global conformal mesh

The method in [6][5] introduced a method, abbreviated as GCM, to accomplish the global conformal parameterization for the genus zero surface. The accomplished meshes are very uniform. The proposed smooth surface can be applied to the GCM meshes. The GCM devised an iteration procedure to optimize a conformal energy function to derive the global mesh. The GCM has two phases in its procedure. The first phase is to apply the barricentric mapping algorithm and the second phase is to apply the conformal mapping algorithm. The procedure starts with a given mesh with all acute angles in its all mesh holes. With any obtuse angle, the string constant in its energy function will be negative and the constructed harmonic map is not bijective. This given mesh must have all acute triangles in its all mesh holes. It cannot



(a) The model surface M by the smooth algorithm. (b) The checkerboard texture mapping on M . (c) The 2D facial makeup in Chinese opera. (d) The facial texture mapping on M .

Figure 6.



Texture mapping on the Igea's head. (a,b) The checkerboard texture mapping. (c) The 2D facial makeup in Chinese opera. (d) The facial makeup mapping on the Igea's head.

Figure 7.

start with the unorganized cloud patterns X . The GCM requires an explicit given mesh to start its procedure. Another difficulty is that during the optimization procedure, certain triangle may be deformed to a line shape. This will introduce a zero denominator in the formula of the string constant. This constant will approach to infinity and the procedure will not work. To avoid such situation, an extra effort is created to sense a zero denominator and prevent it from happen.

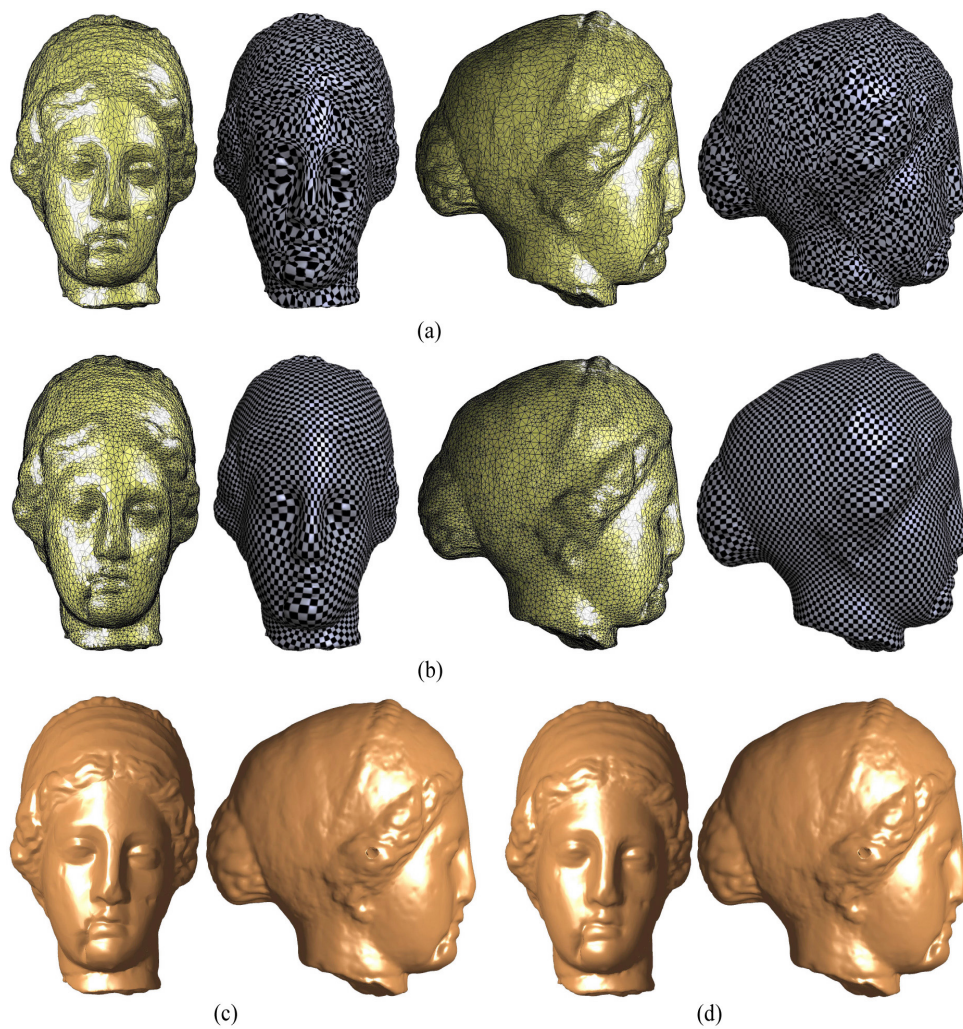
Figures 8 and 9 show the mesh surfaces derived from the obtuse triangulation (a) and the acute triangulation (b) by using the GCM. Figures 8(a) and 9(a) show difficult mappings with obtuse angles in the given meshes. The given obtuse mesh is obtained directly from the pattern cloud X . The acute meshes in Figs. 8(b) and 9(b) are obtained by using the Laplacian smoothing method [4]. The Laplacian smoothing may not derive a mesh with all acute angles. We check the two Laplacian meshes to ensure that they meet the acute criterion and are usable as the given meshes in the GCM. We apply the smooth algorithm to the GCM meshes in Figs. 8(a,b) and 9(a,b) and obtain their smooth surfaces in Figs. 8(c,d) and 9(c,d) respectively. The checkerboard textures in these two figures are obtained by using the same stereographic projection as that used in Fig. 6.

The meshes in Figs. 8(a,b) have $N = 12963$ vertices and $R = 25922$ faces. The meshes in Figs. 9(a,b) $N = 12963$ vertices and $R = 25921$

faces. The step length, δt , in the GCM is set to a value 0.01 in barricentric phase and to a value 10^{-6} in conformal mapping algorithm. The total number of the learning epoch is roughly $epoch_b \approx 900000$ for the barricentric mapping and $epoch_c \approx 90000$ for the conformal mapping. With this epoch number the harmonic energy can reach the minimum. The GCM meshes in Figs. 9(a,b) have serious distortions in the bunny's ears. See Fig. 9(e) for the detailed parameterization at the ears. Figures 8(c,d) show a dense mesh with $N^{new} = 128000$ vertices by using the smooth algorithm. Figures 9(c,d) show a dense mesh with $N^{new} = 128000$ vertices by applying the smooth algorithm. Note that parts of the ear in Figs. 9(c,d) are deformed. This is because the ears are shrinking in the parameterization where the dense mesh N^{new} , shown in red grid in 9(e), cannot cover (make up for) the parts).

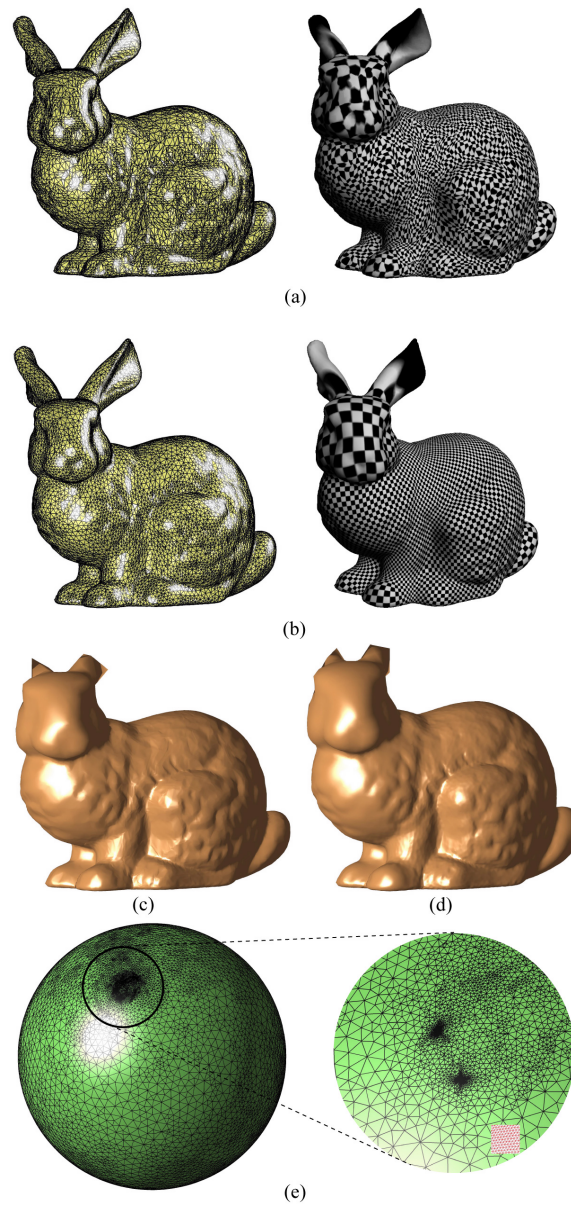
4. Summary

The smooth algorithm accomplishes the curved smooth surface instead of the flat triangle surface obtained from the CSM. The CSM in [11] was designed, originally, to trace the system state which changes continuously and to resolve various severe competitions among finite neurons in the self-organizing map (SOM). The SOM with finite neurons cannot be



Igea model surface by the GCM. (a) The given mesh contains obtuse triangles and the constructed mapping has serious distortion. (b) The given mesh has all acute triangles and the constructed mapping is very uniform. (c) The smooth surface, M , applied to the GCM mesh in (a). (d) The smooth surface, M , applied to the GCM mesh in (b).

Figure 8.



Bunny mesh by the GCM. (a) The given mesh contains many obtuse triangles and the constructed mapping has serious distortion. (b) The given mesh has all acute triangles and the constructed mapping is very uniform. (c) The smooth surface, M , applied to the GCM mesh in (a). (d) The smooth surface, M , applied to the GCM mesh in (b). (e) The parameterization of (b) on the sphere. Right side of (c) is a detail view of bunny's ears and the red grid is a portion of \mathbb{N}^{new} .

Figure 9.

used for monitoring the continuous state. The folded mesh in the SOM can be indicated and resolved by the negative values of the Jacobian of the mapping function [12]. The CSM can save and accommodate fine textures in the map. The CSM with flat triangle surface in 3D [14] has ambiguous resolution on the triangle edges. So, the 3D surface S^Δ and M^Δ are not suitable for tracing the continuous state. The surface S and M will do. Note that the CSM [11] in 2D flat seamless plane does not have such ambiguous problem.

Instead of a surface with flat triangles, a curved smooth parameterization for unorganized data patterns is accomplished for the model surface. This smooth surface is mapped from the sphere surface and serves as a kind of interpolation for the CSM mesh. Since the sphere surface possesses well behaved smooth properties, we expect such mapping can carry the full extent of these beautiful properties to the model surface.

Texture mapping is a direct application of it. The proposed algorithm can be additively applied to many meshes obtained by existing methods. Potential applications are the brain-to-brain registration, consistent parameterization [1][17], facial expression synthesis, deformable object simulation, and computing geodesic path on a model surface. The parameterization for higher genus is also under our study [5][6].

A refined model surface can be obtained by further determining a convex type or a concave type shape for each Δ_w^r instead of mapping only a convex type $\widehat{\Delta}_n^r$ to the part of the model surface $\widehat{\Delta}_w^r$. This means that one can determine the type from the data patterns belong to each Δ_w^r and use this type and the types surrounding Δ_w^r to decide a smooth type for the Δ_w^r . We can isolate an area on M^Δ which contains the same type in its all Δ_w^r . The border triangles between two different type areas will be set flat triangles, that is, $\widehat{\Delta}_w^r = \Delta_w^r$. A concave surface can be obtained by reversing the unit normal vectors of the triangles. The boundary curves should be kept continuous in this refine construction.

References

1. Asirvatham A, Praun E, Hoppe H (2005) Consistent spherical parameterization. In: International Conference on Computational Science (2), pp 265-272
2. Coxeter HSM (1969) Introduction to Geometry, 2nd edn. Wiley, New York
3. Dinh HQ, Turk G (2000) A sampling of surface reconstruction techniques. Graphics, Visualization, and Usability Center, Georgia Institute of Technology, GVU-00-28

4. Field DA (1988) Laplacian smoothing and delaunay triangulations. *Communications in Applied Numerical Methods* 4:709-712
5. Gu X, Yau ST (2002) Computing conformal structures of surfaces. *Communications in Information and Systems* 2(2):121-146
6. Gu X, Yau ST (2003) Global conformal surface parameterization. In: SGP '03: Proceedings of the 2003 Eurographics/ACM SIGGRAPH symposium on Geometry processing, Aachen, Germany, pp 127-137
7. Haker S; Angenent S; Tannenbaum A; Kikinis R; Sapiro G; Halle M (2000) Conformal surface parameterization for texture mapping. *IEEE Transactions on Visualization and Computer Graphics* 6(2):1244-1245
8. Ivriissimtzis IP, Jeong WK, Lee S, Lee Y, Seidel HP (2004) Neural meshes: surface reconstruction with a learning algorithm. Research Report, Max-Planck-Institut Informatik, MPI-I-2004-4-005
9. Jin M, Wang Y, Gu X, Yau ST (2005) Optimal global conformal surface parameterization for visualization. *Communications in Information and Systems* 4(2):117-134
10. Kenner H (1976) *Geodesic math and how to use It*. University of California Press, Berkeley
11. Liou CY, Tai WP (1999) Conformal self-organization for continuity on a feature map. *Neural Networks* 12:893-905
12. Liou CY, Tai WP (2000) Conformality in the self-organization network. *Artificial Intelligence* 116:265-286
13. Tai WP, Liou CY (2000) Image representation by self-organizing conformal network. *The Visual Computer* 16(2):91-105
14. Liou CY, Kuo YT (2005) Conformal self-organizing map for a genus-zero manifold. *The Visual Computer* 21(5):340-353

15. Nehari Z (1952), Conformal Mapping, McGraw-Hill, New York.
16. Phong BT (1975) Illumination for computer generated pictures. Communications of the ACM 18(6):311-317.
17. Praun E, Sweldens W, Schrder P(2001) Consistent mesh parameterizations. In: SIGGRAPH '01: Proceedings of the 28th annual conference on Computer graphics and interactive techniques, New York, NY, USA, pp 179-184
18. Yu Y (1999) Surface reconstruction from unorganized points using self-organizing neural networks. In: Conference Proceedings, IEEE Visualization 99, 99 61-64
19. Cyberware designs, manufactures, and sells standard and custom 3D scanning systems and software (2005), <http://www.cyberware.com/samples/>
20. Stanford Computer Graphics Laboratory, Data archives (2004) <http://www-graphics.stanford.edu/data/>
conformal spherical self-organizing map